High-pressure phase transition in Rb_6C_{60}

R. Poloni,[1,2,*] G. Aquilanti,[1] P. Toulemonde,[2,3] S. Pascarelli,[1] S. Le Floch,[2] D. Machon,[2] D. Martinez-Blanco,[4] G. Morard,[1] and A. San-Miguel[2]

[1]*European Synchrotron Radiation Facility, B.P. 220, F-38043 Grenoble, France*

[2]*LPMCN, CNRS, UMR 5586, Université Claude Bernand–Lyon 1, F-69622 Villeurbanne Cedex, France*

[3]*Département MCMF, Institut Néel, CNRS, Université Joseph Fourier, B.P. 166, F-38042 Grenoble, France*

[4]*Departamento de Física, Universidad de Oviedo, Calvo Soleto, E-33007 Oviedo, Spain*

(Received 10 March 2008; published 22 May 2008)

High-pressure and high-temperature studies have been carried out on the alkali metal–intercalated fullerene system Rb_6C_{60} by performing x-ray diffraction (XRD), x-ray absorption, and Raman spectroscopy measurements. All of these techniques allow the obtaining of complementary information on the high-pressure behavior and evolution of the studied system. In particular, the occurrence of a reversible transition has been clearly identified at around 35 GPa both at 600 K and at room temperature by XRD and Raman spectroscopy, respectively. The XRD data show that the high-pressure phase is compatible with a hexagonal unit-cell structure with $a=8.360(2)$ Å and $c=14.830(7)$ Å at 43 GPa and 600 K. In correspondence with such transition, the Raman spectra exhibit an abrupt change in the frequency of the normal vibrations. By coupling the information obtained with the different experimental techniques, we suggest that the high-pressure structural transition is accompanied by the formation of two-dimensional polymers of C_{60}.

DOI: 10.1103/PhysRevB.77.205433 PACS number(s): 61.48.−c, 61.05.cp, 78.30.Na, 61.05.cj

I. INTRODUCTION

In the last two decades, the study of crystalline C_{60} and its solid compounds has attracted much attention due to the great variety of physical properties observed in these systems both at ambient and extreme conditions of pressure.[1–5] Three-dimensional polymerized C_{60} structures obtained at high-pressure (HP) and high- temperature (HT) conditions[6] have been especially remarked for their exceptional mechanical properties.[5–8] On the other hand, high superconducting critical temperatures have been found for various fullerides with the M_3C_{60} (where M is alkali metal) stoichiometry.[1,9–11] Therefore, the exploration of the P-T phase diagram of alkali metal–intercalated fullerenes is of particular interest and it is the leading motivation of this work. Here, we propose the synthesis of high-dimensional polymerized C_{60} structures starting from the body-centered cubic heavy alkali metal–intercalated fullerenes Rb_6C_{60}, in order to obtain new materials that exhibit both a high hardness and superconducting properties. In fact, it is well known that the presence of heavy alkali ions can catalyze the $sp^2 \rightarrow sp^3$ transition,[12,13] with the application of HP conditions. These new materials, which could consist of polymerized C_{60} molecules connected through small carbon nanocages that have a partial sp^3 character, are expected to exhibit a high electron-phonon coupling parameter responsible for superconductivity, as observed in sp^3 Si clathrates.[14–17]

We have recently shown that the heavy alkali metal–intercalated fullerene compound Cs_6C_{60} displays an exceptional structural stability under high pressures (up to 45 GPa).[18] In particular, we have observed that the intercalation of Cs atoms in the C_{60} crystalline structure allows one to preserve the C_{60} molecule up to a pressure value twice as large as the amorphization pressure of pristine C_{60}. In addition, we have demonstrated that the slight deformation of the C_{60} molecule[19] progressively increases under pressure in M_6C_{60} (M=Rb, Cs).[20] In the case of Rb intercalation, the C_{60} pressure-induced deformation was found to be more important than for Cs intercalation, which suggests that the pressure evolutions of the host-guest interactions for the two fullerides are slightly different.

We have then performed an accurate study on the evolution of the Rb_6C_{60} system, under HP and HT conditions, in order to verify the occurrence of phase transitions leading to the formation of new structures consisting of high-dimensional C_{60} polymers. Additionally, the study of the HP stability of Rb_6C_{60}, compared to that of both pristine C_{60} and Cs_6C_{60}, will allow us to better understand the implication of ionic interactions and of the pressure-induced deformation of the C_{60} molecule on the structural stability of these systems. X-ray diffraction (XRD), x-ray absorption (XAS), and Raman spectroscopy have been used to explore the HP behavior of both the long range and the local structure of the system.

II. EXPERIMENTAL DETAILS

Rb_6C_{60} powder compounds were prepared by mixing stoichiometric amounts of C_{60} (99.95+% purity) with Rb (99.98% purity) in an inert atmosphere. The final reaction was obtained by annealing the mixed powder in a sealed quartz tube at 500 K for a month. The good quality of the sample was checked by XRD and was reported in Ref. 20. HP-HT XRD and XAS experiments were performed at the European Synchrotron Radiation Facility (ESRF, Grenoble, France) by using diamond anvil cells with the x-ray beam traversing two diamonds of 450 μm culet and 2.5 mm height.

Energy dispersive XAS measurements were performed at the insertion device ID24 beamline[21,22] in transmission geometry. A curved Si(111) crystal polychromator coupled to two undulators through a Kirkpatrick-Baez optical system horizontally focused the beam to 10 μm full width at half

maximum (FWHM). A Si-coated mirror was used to vertically refocus the beam down to 10 μm FWHM.

Angular dispersive XRD experiments were performed at the insertion device ID27 beamline[23] by angle-resolved measurements. Monochromatic beams with wavelengths $\lambda = 0.3738$ Å and $\lambda = 0.2647$ Å for HT and room temperature (RT) measurements, respectively, were selected by using a Si(111) monochromator and focused on the sample by using multilayer mirrors in the Kirkpatrick-Baez geometry. The focal spot size was 7×7 μm^2 (FWHM). The diffraction patterns were recorded on a fast large area scanning MAR345 image plate and were analyzed by using the FIT2D (Ref. 24) software package. The sample to detector distance and the image plate tilt angles were precisely calibrated by using a silicon standard located at the sample position.

HP and RT Raman measurements were recorded by using a Jobin Yvon HR-800 LabRAM spectrometer with double-notch filtering and an air cooled charge-coupled device detector (ENS, Lyon). The spectrometer was used in the backscattering geometry. The laser beam (514.5 nm exciting lines of an Ar^+ laser) was focused down to a 2 μm spot on the sample and the backscattered light was collected through the same objective. High resolution spectra (~ 0.5 cm^{-1}) have been collected at RT. Due to the unavoidable backward scattering through the diamond of the high-pressure cell, we did not collect data in the frequency shift region around 1332 cm^{-1} because it was covered by the very strong diamond peak. The optimum laser power was found to be 5 mW, which was directly measured before the high-pressure cell.

For all of the experiments, the pressure was measured *in situ* before and after each measurement by using the R1 fluorescence emission of a ruby chip[25] placed into the gasket hole. We used LiF as the pressure transmitting medium for the HP-HT XRD measurements and NaCl for the HP-RT XRD and Raman spectroscopy measurements. No pressure transmitting medium was used during the XAS measurements in order to provide a more suitable sample thickness for a good signal-to-noise ratio.

The HT conditions for the XAS and XRD experiments were achieved by external resistive heating and the temperature was measured by using a thermocouple placed on the back of one diamond. For the HP-HT XAS and XRD experiments we used a Re gasket with a 100 μm diameter hole, while for the HP-RT temperature Raman measurements we used a stainless steel gasket with a 100 μm diameter hole.

III. EXPERIMENTAL RESULTS

A. X-ray diffraction

At ambient conditions, the Rb_6C_{60} system exhibits a body-centered cubic (bcc) structure ($Im\bar{3}$ space group)[26,27] wherein the fullerene molecules are centered on bcc Bravais lattice sites and the alkali metal atoms occupy all of the 12 available tetrahedral sites of the host lattice. At RT and ambient pressure (AP), the value of the lattice parameter of the Rb_6C_{60} system ($a = 11.54 \pm 0.2$ Å) obtained from our XRD analysis is in agreement with that reported in the literature.[26,28]

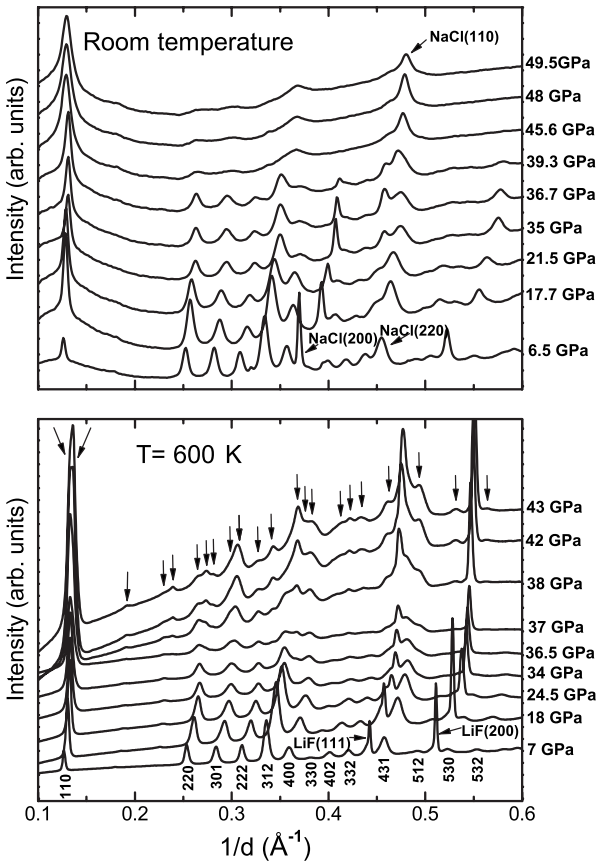

FIG. 1. Upper panel: HP-RT XRD patterns of Rb_6C_{60} and NaCl (used as the pressure transmitting medium), normalized for acquisition time and collected at $\lambda = 0.2647$ Å. The $B1 \rightarrow B2$ phase transition of NaCl is also observed at around 39 GPa (Ref. 44). Lower panel: HT (600 K) and HP XRD patterns of Rb_6C_{60} and LiF (used as the pressure transmitting medium), normalized to LiF(111) Bragg reflection intensity and collected at $\lambda = 0.3738$ Å. All data are reported without background subtraction. All Bragg reflections associated with the high-pressure phase are indicated by the vertical arrows in the XRD pattern collected at 43 GPa.

We studied the evolution of the solid structure of Rb_6C_{60} as a function of pressure both at HT (600 K) and at RT. We performed XRD measurements at RT and HT (600 K) in the pressure range [AP:49.5] GPa and [7:43] GPa, respectively. The XRD patterns were collected after each pressure increase by about 1.5 GPa. In Fig. 1, we report some selected XRD patterns as a function of pressure at room temperature (upper panel) and at 600 K (lower panel).

The data collected at RT as a function of pressure show a reversible discontinuity in the width of the Bragg reflections starting from 45.6 GPa, preventing us to establish the nature of the structural changes occurring in that pressure range. The data set collected at 600 K displays a clear first order phase transition of Rb_6C_{60} toward a lower-symmetry structure corresponding to the appearance of additional Bragg reflections, starting at around 35 GPa. We observe that the transition is accompanied by an increase in the background intensity that could be associated with the presence of structural disorder in the high-pressure phase. At 43 GPa, the highest measured pressure, the phase transition was complete.

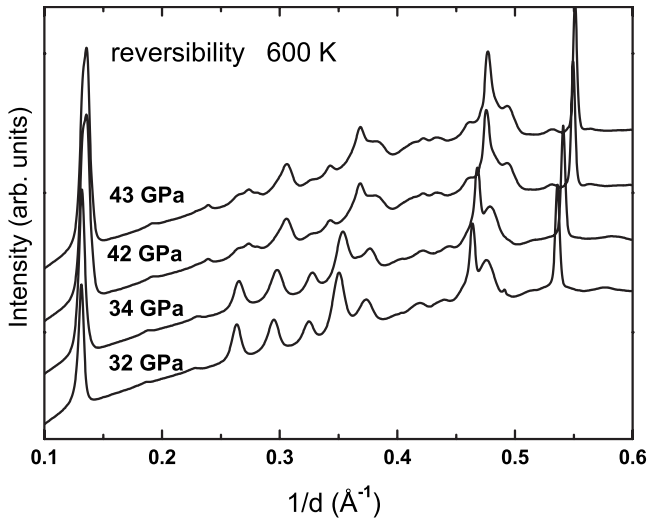

FIG. 2. XRD data collected on Rb_6C_{60} at 600 K, from the highest measured pressure (43 GPa) down to 32 GPa during pressure release. The observed transition is reversible and the cubic phase is back at 32 GPa. The data are normalized to the LiF(111) Bragg reflection intensity.

Two different experiments were performed to study the transition's reversibility dependence on the thermodynamic path. In the first experiment, the pressure was released at a high temperature and the sample at AP was then cooled down to RT. In the second experiment, the temperature was decreased to RT at HP and then the pressure was released to AP.

In both experiments, the transition was observed to be reversible but with different hysteresis ranges. The body-centered cubic phase was back at 32 GPa and at 11 GPa in the former and latter cases, respectively. The patterns collected during the pressure release performed at 600 K are shown in Fig. 2.

Data were analyzed by using the FULLPROF package[29] before and after the phase transition. The unit-cell parameters and profile shape parameters were independently fitted by using the Le Bail method. A dichotomy method was employed for indexing the powder diffraction pattern after the transition by using the DICVOL program.[30] The new structural phase of Rb_6C_{60} was found to be compatible with a hexagonal unit-cell structure. Among the different solutions, only the hexagonal cell was found to be compatible with a network built of C_{60} molecules. The resulting lattice parameters at 43 GPa and 600 K are $a=8.360(2)$ Å and $c=14.830(7)$ Å, giving a c/a ratio of 1.774, which is only 8% larger than the ideal c/a axial ratio for hexagonal close-packed crystal structures (1.633). The corresponding Le Bail fit, which was performed by imposing the $P6/mmm$ space group, is shown in Fig. 3 and gives the R factor $R_{wp}=6.5\%$ ($\chi^2=0.29$). In Fig. 4, the evolution of the unit-cell volume of Rb_6C_{60} as a function of pressure exhibits a volume collapse of 24% at the phase transition from the bcc to the hexagonal phase. Unfortunately, due to the data quality at high pressure, a Rietveld-type refinement was not possible, preventing us from obtaining information on atomic positions within the unit cell.

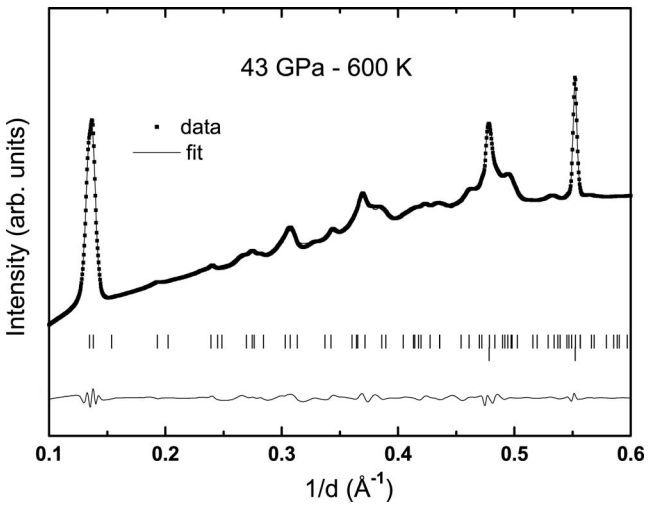

FIG. 3. Le Bail fit of the XRD pattern collected on Rb_6C_{60} at 43 GPa and 600 K ($R_{wp}=6.5\%$ and $\chi^2=0.29$). The ticks correspond, from bottom to top, to LiF and Rb_6C_{60}. The data and the fit curve are presented as dotted and solid lines, respectively. The lower line corresponds to the residual pattern.

B. Raman spectroscopy

Raman spectra were collected at ambient temperature as a function of pressure from 0.3 to 40.3 GPa. Only part of the collected spectra are reported in Fig. 4 for clarity. The Raman spectrum at 0.3 GPa shows the presence of a shoulder in the $A_g(2)$ mode due to the presence of an impurity that was also found on the gasket.

For the isolated C_{60} with I_h symmetry, only 10 of the 46 Raman lines are Raman active ($2A_g+8H_g$). For the fully doped M_6C_{60} compound with T_h^5 symmetry, calculations[31] have shown that each of the five-dimensional Raman active H_g modes appearing in the isolated C_{60} molecule split into a two-dimensional E_g mode and a three-dimensional T_g mode. Moreover, the $3T_{1g}$, $4T_{2g}$, and $6G_g$ modes in the I_h symmetry

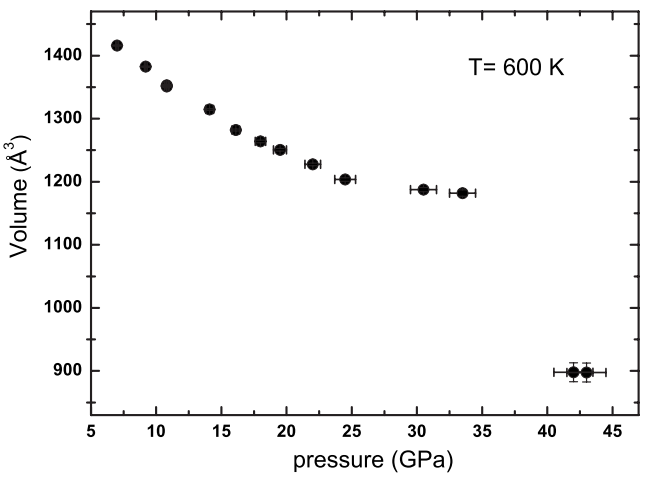

FIG. 4. Pressure evolution of the unit-cell volume of Rb_6C_{60} from 3 to 43 GPa, at 600 K. In correspondence to the bcc $\rightarrow$hexagonal phase transition, this volume exhibits a 24% volume collapse from 34 to 42 GPa.

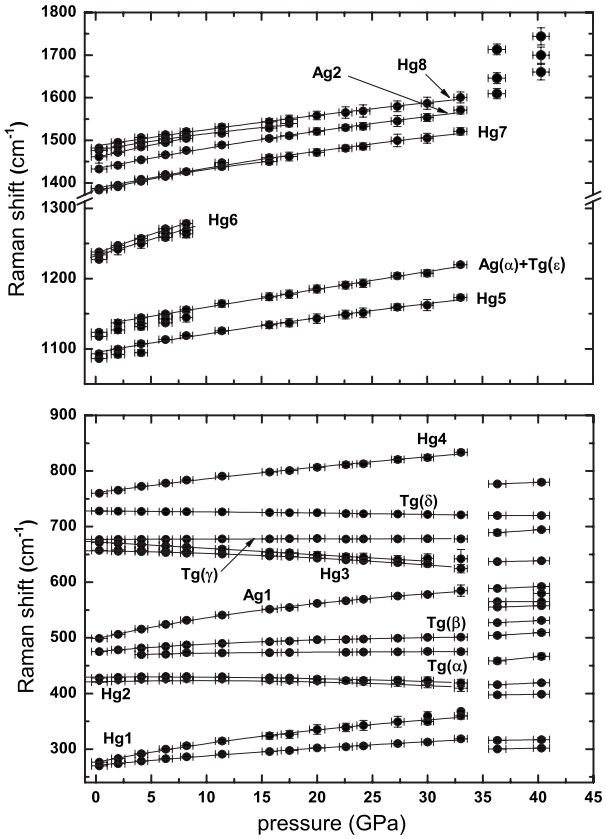

FIG. 5. Low-frequency (lower panel) and high-frequency (upper panel) Raman modes pressure evolution. The solid lines correspond to least-square fits to a parabolic-type pressure dependence for all modes before the transition at 36.3 GPa. The horizontal error bars represent the pressure uncertainty estimated from the Lorentzian width of the R1 ruby line; the vertical error bars correspond to the HWHM of each Raman mode.

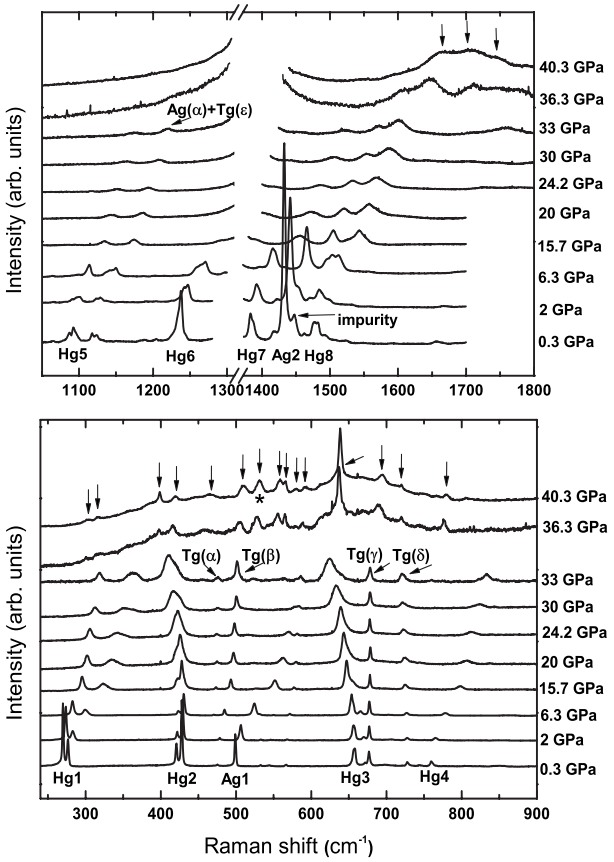

FIG. 6. Pressure evolution of the low-frequency (lower panel) and high-frequency (upper panel) Raman spectra of Rb_6C_{60} at room temperature. All data are reported with no background subtraction. The mode intensity has been normalized to the $T_g(\gamma)$ and $H_g(8)$ intensities for the low- and high-frequency spectra, respectively. After the transition, both the low-frequency and the high-frequency data have been normalized to the intensity of the mode labeled with an asterisk (*). The Raman modes observed after the transition are indicated by the vertical arrows in the spectrum collected at 40.3 GPa.

should become weakly Raman active upon changing their symmetries into $3T_g$, $4T_g$, and $6(A_g+T_g)$, respectively.

Nevertheless, the Raman spectrum of Rb_6C_{60} measured at ambient pressure and room temperature and previously reported by Zhou *et al.*[32] showed that only ten main modes were Raman active, corresponding to the ten Raman active modes of the isolated molecule. In addition, Zhou *et al.*[32] observed that five of the eight H_g modes [$H_g(1)$, $H_g(2)$, $H_g(3)$, $H_g(5)$, and $H_g(7)$] were split into doublets by a measurable amount.

In the present work, the Raman spectrum collected at 0.3 GPa is in good agreement with Ref. 32, with the $H_g(1)$, $H_g(2)$, $H_g(3)$, $H_g(5)$, and $H_g(7)$ modes split into doublets. However, in the present high-pressure study, we also observe six completely new Raman lines and three additional partners in doublets, corresponding to the $H_g(4)$, $H_g(6)$, and $H_g(8)$ modes, as also observed in our recent Raman study on Cs_6C_{60}.[18] Numerous other Raman active modes that were anticipated for solid M_6C_{60} were found to exhibit an insufficient Raman activity.

The pressure evolutions of the frequencies of all of the observed Raman lines are shown in Fig. 5. In Fig. 6, we label the ten intramolecular Raman vibrations that were previously observed as the $2A_g$ and $8H_g$ symmetry modes of the free molecule in order to keep the same nomenclature used in the past. On the other hand, we label the new observed lines with the names of the irreducible representation of the Raman active modes in the Rb_6C_{60} system with T_h^5 symmetry. The symmetry of the six new observed Raman modes has been identified with the help of *ab initio* density functional theory (DFT) calculations as reported in our previous work.[18] Consistently with their calculated symmetry, they are labeled $T_g(\alpha)$, $T_g(\beta)$, $T_g(\gamma)$, $T_g(\delta)$, $T_g(\epsilon)$, and $A_g(\alpha)$ in Fig. 6.

The continuous evolution of the observed Raman modes is interrupted by an abrupt change in the mode frequencies occurring between 33 and 36.3 GPa. We observe the disappearance of the well known Raman intramolecular modes and the appearance of completely new modes both in the low- and high-frequency ranges. This can be reasonably related to a significant change in the nature of the intramolecular covalent bonds between C atoms and/or C-Rb atoms. The observed transition is also accompanied by a change in the background displaying a broad continuum in the frequency range of $300<\omega<800$ cm^{-1}. We also collected Raman

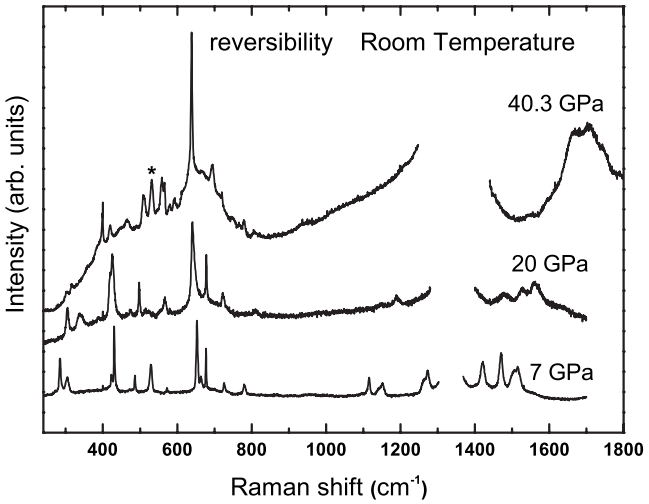

FIG. 7. Raman spectra collected at the highest measured pressure, 40.3 GPa, and during the pressure release, at 20 and 7 GPa, showing the reversibility of the transition. The data at 20 and 7 GPa reported without background subtraction have been normalized to the intensity of the $T_g(\gamma)$ mode, while the spectrum at 40.3 GPa has been normalized to the intensity of the $*$ mode.

spectra during the pressure release at 20 and 7 GPa. These spectra, which are displayed in Fig. 7, evidence the reversibility of the observed transition.

C. X-ray absorption spectroscopy

XAS spectra were collected at the Rb K edge (15.2 keV) as a function of pressure both at RT and HT (600 K). In Fig. 8, we report some of the x-ray absorption near edge structure (XANES) spectra in the pressure range of up to 40 GPa (600 K) and 46 GPa (RT). Due to the unavoidable Bragg reflections from the diamond anvils, data were collected up to 300 eV above the edge, preventing a quantitative extended x-ray absorption fine structure analysis.

In both the RT and the HT experiments, we do not observe any clear modification with pressure of the edge position within the precision of our measurements (± 0.4 eV), which indicates that no clear change in the electronic charge transfer from the alkali metals to molecules can be established.

A continuous and progressive evolution of the XANES signal as a function of pressure is observed at both temperatures. This evolution is characterized by (i) a progressive enlargement of the white line with a slight fall in intensity; (ii) a modification of the shape of the first XANES oscillation: the initial doublet shape gradually shows a decrease in the first peak intensity and globally shifts toward higher energies; (iii) the progressive disappearance of the second oscillation located at around 15.27 keV (at a lower pressure).

For both experiments, a pressure release was performed at RT. Data were collected down to 22 and 15 GPa for the 600 K and RT experiments, respectively. In both cases we observe a similar progressive reversibility of the signal. Figure 9 displays the XANES spectra upon a pressure decrease from 40 to 22 GPa, after cooling the sample down to RT.

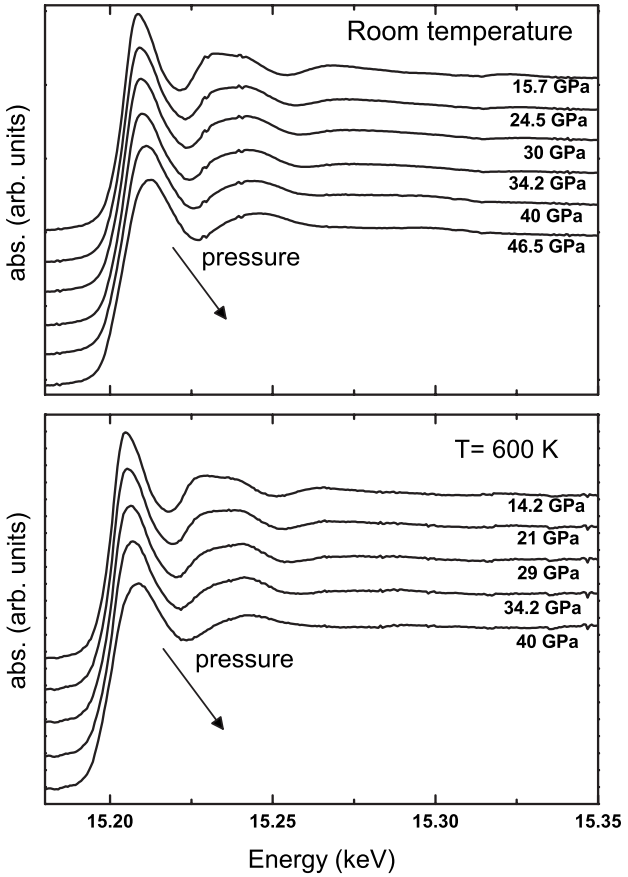

FIG. 8. Rb K-edge XANES spectra of Rb_6C_{60} as a function of pressure at room temperature (upper panel) and at 600 K (lower panel).

IV. DISCUSSION AND CONCLUSIONS

A detailed study on the structural evolution under pressure of the Rb_6C_{60} system has been reported by performing XRD, XAS, and Raman spectroscopy measurements. The occur-

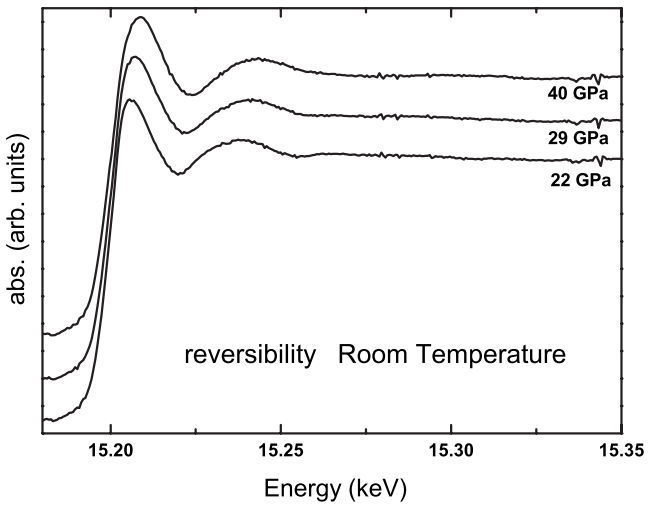

FIG. 9. XANES spectra collected at RT during the pressure release of the sample studied at 600 K. We observe a progressive reversibility of the signal.

rence of a reversible transition, at around 35 GPa, is observed by the XRD and the Raman data, at 600 K and room temperature, respectively. The XAS data show that both the local structure and the electronic configuration around each Rb atom exhibit a progressive and similar change with pressure at both high and room temperatures.

A clear reversible first order phase transition has been observed by XRD, at around 35 GPa at 600 K. Our analysis shows that the new phase is compatible with a hexagonal unit-cell structure, with $a=8.360(2)$ Å and $c=14.830(7)$ Å at 43 GPa and 600 K. Since the C_{60} molecules normally occupy the vertices of the unit cell in all fullerene-based structures, the intermolecular distance in the plane containing the $\vec{a}$ $\vec{b}$ unit-cell vectors is compatible with the presence of covalent bonds between these molecules. In fact, C_{60} polymerization has been observed in both solid C_{60} and fullerides with resulting intermolecular distances between the polymerized molecules in the range of 9.09–9.30 Å at ambient conditions.[33–35] Hence, a possible interpretation of the observed structural change is that the bcc→hexagonal unit-cell symmetry transition is accompanied by the formation of networks of two-dimensional (2D) polymerized C_{60} molecules in the (001) plane of the hexagonal structure. Consequently, in each C_{60}-polymerized plane, the molecule could be covalently linked to its six neighboring molecules, as previously observed by Margadonna *et al.*[34] for the 2D polymerization of pristine C_{60} encountered in the rhombohedral structure. The Raman spectroscopy measurements performed at room temperature show the existence of an important and discontinuous change, at around 35 GPa, in the frequency of the intramolecular normal vibrations.

A possible reason could be the formation of C_{60} polymers, i.e., the formation of covalent bonds between neighboring molecules as a consequence of their pressure-induced vicinity. In addition, the formation of covalent intermolecular bonds and the concomitant change in the intramolecular C-C bondings have been previously observed to be responsible for the breaking of the icosahedral symmetry of C_{60} molecules in the orthorhombic, tetragonal, and rhombohedral structures of polymerized C_{60} (Ref. 36) leading to a strong change in the Raman spectrum. This explanation is compatible with our XRD experiments, which suggests that the origin of the new hexagonal structure is linked to a polymerization process. Also, the formation of reversible covalent bonds between the Rb atoms and the C_{60} fullerenes can be envisaged, as recently observed in Sm_3C_{70} (Ref. 37) and Eu_3C_{70} (Ref. 38) fullerides. In these structures, the rare earth metals bridge two C_{70} molecules, producing C_{70}-Sm-C_{70} dimer structures.

It should be noticed that in the present work, the $A_g(2)$ mode is not observed to shift toward lower wave numbers at the phase transition as expected for the formation of C_{60} polymers in pristine fullerite.[39] This could be related to a strong decrease in the charge transfer between the alkali ions and the C_{60}.[40] In fact, the $A_g(2)$ mode frequency has been observed to depend on both the number of intermolecular bonds and the charge transfer. A similar observation has been reported for 2D polymerized $Li_xNa_{(4-x)}$-intercalated fullerenes.[35] In that work, the $A_g(2)$ mode is found at 1460 cm^{-1}, a value typical of undoped one-dimensional C_{60} chains.

Both the XRD and the Raman data exhibit an increase in the background intensity after the transition, which probably indicates the presence of structural disorder in the HP phase. The reversibility of the background intensity in both the Raman and the XRD measurements clearly indicates that such disorder is not linked to the loss of a fraction of molecular cages. Although the application of pressure on the Rb_6C_{60} system leads to a compression and a slight deformation of C_{60},[20] the molecular character of the system is preserved during the present study. In addition, the reversibility of both the Raman and the XRD data rule out the possibility of a compositional disorder at high pressure. The formation of different stoichiometric compounds at the transition seems unlikely with respect to the observed reversibility. In fact, we do not observe frequency changes in the majority of the Raman modes between the spectra recorded during decompression and during compression at similar pressures. Nor are additional Bragg reflections observed upon decompression. Nevertheless, nanometer scale segregation in the high-pressure phase, such as stacking faults in the 2D structure, cannot be excluded, as they could allow reversibility and also explain the observed disorder in the high-pressure phase. Also, clustering of Rb atoms in the HP phase can reasonably be excluded by the XAS data since the presence of direct Rb-Rb interactions would dramatically modify the Rb *K*-edge absorption spectrum.

The XRD data collected at RT show a discontinuous broadening of the Bragg reflections starting from 45.6 GPa, preventing us from clarifying the nature of the structural changes occurring in that pressure range. Such an increase in peak width, which is more important at RT than it is at HT, could be attributed to the presence of structural strains that build up and cannot relax in the absence of high-temperature conditions. In addition, a better sample crystallization at 600 K compared to that at RT could be also responsible for the observed difference in the width of the Bragg reflections. This observation is compatible with the complexity of the polymerization process in fullerenes that was already observed in pristine C_{60} (Ref. 41), reinforcing the idea that the observed high-pressure hexagonal phase is associated with the formation of C_{60} polymers. Moreover, the limitation in long-range crystallization of the high-pressure phase in the RT experiment does not affect the changes in the local symmetry of the system. This is consistent with the results obtained by Raman spectroscopy and by XAS, which are local probes. In addition, since in the Rb_6C_{60} system, the rotation of molecules is hampered by the presence of a strong ionic interaction between the alkali atoms and the C_{60} fullerene, a different scenario wherein different structural phases existing at RT and at 600 K appears to be less probable.

The evolution of the XANES spectra between ambient pressure and 46 GPa shows the occurrence of a continuous and important evolution of the local structure around each alkali metal atom. The comparison between the progressive modification of the XAS data observed at 600 K and at RT indicates that the phase transition and the pressure-induced increase in the Bragg reflection width are accompanied by the same pressure evolution of the local structure and elec-

tronic configuration around each Rb atom. This reinforces our hypothesis of observing the same phase transition at both RT and HT. Nevertheless, the pressure evolution of the XANES signal alone is insufficient to clarify whether the observed change in the local structure could be associated with a phase transformation. Additional HT and HP studies on Rb_6C_{60} would be necessary to definitively identify the high-pressure phase observed in this work. XRD measurements at a low temperature after quenching the sample from a high temperature could provide higher quality data compared to those reported in this study.

An important remark concerning the high-pressure stability of the Rb_6C_{60} system must be made. Raman spectroscopy and XRD, showing the existence of a transition at around 35 GPa, prove the lower pressure stability of the molecular character of Rb_6C_{60} compared to the isostructural Cs_6C_{60} compound, where a continuous evolution of the Raman active modes has been observed up to 45 GPa.[18] This behavior is concomitant with a more pronounced pressure-induced distortion of C_{60} in Rb_6C_{60} than in Cs_6C_{60}. Nevertheless, both fullerides show a much higher pressure stability of the molecular character of the system compared to the solid C_{60}, which was observed to amorphize at 22 GPa.[42,43] Subsequently, the fundamental role of Coulomb interactions on the pressure evolution of the M_6C_{60} systems can be reasonably assumed. We therefore infer that the presence of such ionic interactions could be responsible for the high-pressure stabilization of the C_{60} molecules. In conclusion, the present detailed study on the HP and HT structural behavior of the Rb_6C_{60} compound provides fundamental information concerning the synthesis of high-dimensional polymerized C_{60} materials.

ACKNOWLEDGMENTS

The authors thank M. Mezouar for allocation of internal time and G. Montagnac and H. Cardon for assistance during the Raman experiments. R.P. acknowledges L. Marques and K. Prassides for helpful discussions. Beamtime was allocated under Proposal No. HE2468 at ID24 and ID27, ESRF.

*Present address: Institut de Ciència de Materials de Barcelona (CSIC), Campus de la UAB, E-08193 Bellaterra, Barcelona, Spain.

[1] R. M. Fleming, A. P. Ramirez, M. J. Rosseinsky, D. W. Murphy, R. C. Haddon, S. M. Zahurak, and A. V. Makhija, Nature (London) **352**, 787 (1991).
[2] A. F. Hebard, M. J. Rosseinsky, R. C. Haddon, D. W. Murphy, S. H. Glarum, T. T. M. Palstra, A. P. Ramirez, and A. R. Kortan, Nature (London) **350**, 600 (1991).
[3] B. Sundqvist, Adv. Phys. **48**, 1 (1999).
[4] L. Marques, M. Mezouar, J.-L. Hodeau, M. Núñez-Regueiro, N. R. Serebryanaya, V. A. Ivdenko, V. D. Blank, and G. A. Dubitsky, Science **283**, 1720 (1999).
[5] V. D. Blank, S. G. Buga, G. A. Dubitsky, N. R. Serebryanaya, M. Y. Popov, and B. Sundqvist, Carbon **36**, 319 (1998).
[6] M. Mezouar, L. Marques, J.-L. Hodeau, V. Pischedda, and M. Núñez-Regueiro, Phys. Rev. B **68**, 193414 (2003).
[7] V. D. Blank, V. M. Levin, and N. R. Serebryanaya, JETP **87**, 741 (1998).
[8] S. Yamanaka, A. Kubo, K. Inumaru, K. Komaguchi, N. S. Kini, T. Inoue, and T. Irifune, Phys. Rev. Lett. **96**, 076602 (2006).
[9] K. Prassides, C. Christides, I. M. Thomas, J. Mizuki, K. Tanigaki, I. Hirosawa, and T. W. Ebbesen, Science **263**, 950 (1994).
[10] T. T. M. Palstra, O. Zhou, Y. Iwasa, P. E. Sulewski, R. M. Fleming, and B. R. Zegarski, Solid State Commun. **93**, 327 (1994).
[11] S. Margadonna and K. Prassides, J. Solid State Chem. **168**, 639 (2002).
[12] M. M. Abd-Elmeguid, H. Pattyn, and S. Bukshpan, Phys. Rev. Lett. **72**, 502 (1994).
[13] C. M. Sung and M. F. Tai, Int. J. Refract. Met. Hard Mater. **15**, 237 (1997).
[14] D. Connétable, V. Timoshevskii, B. Masenelli, J. Beille, J. Marcus, B. Barbara, A. M. Saitta, G.-M. Rignanese, P. Mélinon, S. Yamanaka, and X. Blase, Phys. Rev. Lett. **91**, 247001 (2003).
[15] X. Blase, C. Adessi, and D. Connétable, Phys. Rev. Lett. **93**, 237004 (2004).
[16] N. Breda, R. A. Broglia, G. Coló, G. Onida, D. Provasi, and E. Vigezzi, Phys. Rev. B **62**, 130 (2000).
[17] A. San Miguel and P. Toulemonde, High Press. Res. **25**, 159 (2005).
[18] R. Poloni, D. Machon, M. V. Fernandez-Serra, S. Le Floch, S. Pascarelli, G. Montagnac, H. Cardon, and A. San-Miguel, Phys. Rev. B **77**, 125413 (2008).
[19] W. Andreoni, F. Gygi, and M. Parrinello, Phys. Rev. Lett. **68**, 823 (1992).
[20] R. Poloni, M. V. Fernandez-Serra, S. Le Floch, S. De Panfilis, P. Toulemonde, D. Machon, W. Crichton, S. Pascarelli, and A. San-Miguel, Phys. Rev. B **77**, 035429 (2008).
[21] M. Hagelstein, A. San Miguel, T. Ressler, A. Fontaine, and J. Goulon, J. Phys. IV **7**, 303 (1997).
[22] S. Pascarelli, O. Mathon, and G. Aquilanti, J. Alloys Compd. **362**, 33 (2004).
[23] M. Mezouar, W. A. Crichton, S. Bauchau, F. Thurel, H. Witsch, F. Torrecillas, G. Blattmann, P. Marion, Y. Dabin, J. Chavanne, O. Hignette, C. Morawe, and C. Borel, J. Synchrotron Radiat. **12**, 659 (2005).
[24] D. P. Hammersley, S. O. Svensson, M. Hanfland, A. N. Fitch, and D. Hausermann, High Press. Res. **14**, 235 (1996).
[25] R. A. Forman, P. J. Piermarini, J. P. Barnett, S. Block, and R. A. Forman, Science **176**, 284 (1972).
[26] O. Zhou, J. E. Fischer, N. Coustel, S. Kycia, Q. Zhu, A. R. McGhie, W. J. Romanow, J. P. McCauley, A. B. Smith, and D. E. Cox, Nature (London) **351**, 462 (1991).
[27] O. Zhou and D. E. Cox, J. Phys. Chem. Solids **53**, 1373 (1992).
[28] A. A. Sabouri-Dodaran, M. Marangolo, Ch. Bellin, F. Mauri, G. Fiquet, G. Loupias, M. Mezouar, W. Crichton, C. Hérold, F. Rachdi, and S. Rabi, Phys. Rev. B **70**, 174114 (2004).
[29] J. Rodriguez-Carvajal, Physica B **192**, 55 (1993).
[30] D. Louër and R. Vargas, J. Appl. Crystallogr. **15**, 542 (1982).
[31] G. Dresselhaus, M. S. Dresselhaus, and P. C. Eklund, Phys. Rev.

B **45**, 6923 (1992).
[32] P. Zhou, K.-A. Wang, Y. Wang, P. C. Eklund, M. S. Dresselhaus, G. Dresselhaus, and R. A. Jishi, Phys. Rev. B **46**, 2595 (1992).
[33] B. Verberck, H. Michel, and A. V. Nikolaev, J. Chem. Phys. **116**, 10462 (2002).
[34] S. Margadonna, D. Pontiroli, M. Belli, M. R. T. Shikora, and M. Brunelli, J. Am. Chem. Soc. **126**, 15032 (2004).
[35] R. Röding, T. Wågberg, and B. Sundqvist, Chem. Phys. Lett. **413**, 157 (2005).
[36] A. M. Rao, P. C. Eklund, J.-L. Hodeau, L. Marques, and M. Núñez-Regueiro, Phys. Rev. B **55**, 4766 (1997).
[37] D. H. Chi, Y. Iwasa, X. H. Chen, T. Takebonu, T. Ito, T. Mitani, E. Nishibori, M. Takata, M. Sakata, and Y. Kubozono, Chem. Phys. Lett. **359**, 177 (2002).
[38] T. Takenobu, D. H. Chi, S. Margadonna, K. Prassides, Y. Kubozono, A. N. Fitch, K. Kato, and Y. Iwasa, J. Am. Chem. Soc. **125**, 1897 (2003).
[39] B. Sundqvist, Struct. Bonding (Berlin) **109**, 85 (2004).
[40] We have studied the electronic evolution of the Rb_6C_{60} compound as a function of pressure by first principles DFT calculations. We observed that the charge transfer from the Rb ions to C_{60} gradually decreases with pressure. More remarkably, an instability of the bcc lattice of Rb_6C_{60} was observed at high pressures and is accompanied by an abrupt decrease in the charge transfer; R. Poloni, Ph.D. thesis, University of Lyon, 2007.
[41] R. Moret, Acta Crystallogr., Sect. A: Found. Crystallogr. **61**, 62 (2005).
[42] M. Núñez-Regueiro, P. Monceau, and J.-L. Hodeau, Nature (London) **355**, 237 (1992).
[43] D. W. Snoke, Y. S. Raptis, and K. Syassen, Phys. Rev. B **45**, 14419 (1992).
[44] N. Sata, G. Shen, M. L. Rivers, and S. R. Sutton, Phys. Rev. B **65**, 104114 (2002).